LABORATÓRIO DE INSTRUMENTAÇÃO E
FÍSICA EXPERIMENTAL DE PARTÍCULAS

LIP / 95–06
14 Jun 1995

Muon pair and vector meson cross-sections in p-W and S-U collisions at 200 GeV/nucleon

M.C. Abreu[4,a], C. Baglin[1], A. Baldisseri[1,♭], A. Baldit[2], M. Bedjidian[8], P. Bordalo[4,b], A. Bussière[1], J. Castor[2], T. Chambon[2], B. Chaurand[6], D. Contardo[8], E. Descroix[8], A. Devaux[2], O. Drapier[8], B. Espagnon[2], J. Fargeix[2], R. Ferreira[4,♯], P. Force[2], J. Gago[4,b], C. Gerschel[5], P. Gorodetzky[7], J.Y. Grossiord[8], A. Guichard[8], J.P. Guillaud[1], R. Haroutunian[8], D. Jouan[5], L. Kluberg[6], R. Kossakowski[1], G. Landaud[2], P. Liaud[1], C. Lourenço[4,♯], R. Mazini[7], S. Papillon[5], L. Peralta[4,a], J.R. Pizzi[8], C. Racca[7], S. Ramos[4,b], A. Romana[6], S. Silva[4], P. Sonderegger[3,b], X. Tarrago[5], J. Varela[4,b♯]

NA38 Collaboration

Abstract

Muon pair production is studied in $p-W$ and $S-U$ collisions at 200 GeV per nucleon, as a function of transverse momentum $P_{T\mu\mu}$. The inclusive $\rho+\omega$ and ϕ differential cross-sections $d\sigma/dP_T$ are measured in the dimuon decay channel, for $P_T \geq$0.6 GeV/c, in the central rapidity region, 3.0$\leq y \leq$4.0. Assuming the power law A-dependence $\sigma = \sigma_0(A_{beam} \cdot A_{target})^\alpha$, the study of the integrated cross-sections for $p-W$ and $S-U$ collisions leads to $\alpha_{\rho+\omega} = 1.00 \pm 0.02 \pm 0.07$ and $\alpha_\phi = 1.23 \pm 0.03 \pm 0.05$, showing clear evidence of ϕ enhancement in $S-U$ interactions as compared to $p-W$ collisions.

Accepted to be published in Physics Letters B

1) Laboratoire d'Annecy-le-Vieux de Physique des Particules, IN2P3-CNRS, B.P. 110, F-74941 Annecy-le-Vieux Cedex, France
2) Laboratoire de Physique Corpusculaire de Clermont-Ferrand, IN2P3-CNRS et Université Blaise Pascal, F-63177 Aubière Cedex, France
3) CERN, CH-1211 Geneva 23, Switzerland
4) LIP, Av. Elias Garcia 14, P-1000 Lisbon, Portugal
5) Institut de Physique Nucléaire, IN2P3-CNRS et Université de Paris-Sud, F-91406 Orsay Cedex, France
6) Laboratoire de Physique Nucléaire des Hautes Energies, Ecole Polytechnique, IN2P3-CNRS, F-91128 Palaiseau Cedex, France
7) Centre de Recherches Nucléaires, IN2P3-CNRS et Université Louis Pasteur, BP 20, F-67037 Strasbourg Cedex, France
8) Institut de Physique Nucléaire de Lyon, IN2P3-CNRS et Université Claude Bernard, 43 Boulevard du 11 Novembre 1918, F-69622 Villeurbanne Cedex, France
a) Also at FCUL, Universidade de Lisboa, Lisbon, Portugal.
b) Also at IST, Universidade Técnica de Lisboa, Lisbon, Portugal.
♭) Present address DAPNIA CEN Saclay, France.
♯) Present address CERN Geneva, Switzerland.

1 INTRODUCTION

Lepton pair production in ultrarelativistic heavy ion collisions is a potential source of signals related to the phase transition of ordinary nuclear matter into the Quark Gluon Plasma state [1].

In this article, we report on dimuon production cross-sections as a function of mass and transverse momentum, in $p-W$ and $S-U$ collisions at 200 GeV/nucleon, in the central rapidity region. We also discuss the A^{α} dependence of $\rho+\omega$ and ϕ cross-sections and its behaviour as a function of P_T. The results on the production of ϕ and unseparated $\rho+\omega$ resonances as a function of the dimuon transverse mass $M_{T\mu\mu}$ and energy density ϵ of the collision are discussed in a subsequent paper [2].

2 EXPERIMENTAL SET-UP

The NA38 apparatus [3] consists mainly of a muon spectrometer, accepting muon pairs in the rapidity range $2.8< y <4.1$.

The present analysis corresponds to data taken with dedicated configurations of the detector shown in Fig. 1. With respect to the setup used to study the J/ψ, as described in [3], the study of the ρ, ω and ϕ resonances requires a better mass resolution while keeping low the level of combinatorial background due to meson decays. This is obtained by using light material absorbers, which remove about 10 radiation lengths from the very beginning of the trajectories of the muons accepted by the spectrometer.

In the $S-U$ configuration, the active target system is made of 10 subtargets, corresponding to 20% total interaction length. It identifies the subtarget of the primary interaction and flags reinteractions of spectator fragments when they occur. The electromagnetic energy of the reaction is measured by the calorimeter described in [3], with its inner part replaced by a 12 cm Al_2O_3 absorber [1)]. The calorimeter is followed by an absorber made of 40 cm of Al_2O_3 and 480 cm of carbon. Two different beam monitors are used to count and identify the incoming ions: the beam hodoscope (BH), which is also used to fight the beam pile-up, and the beam-in (BI) detector, which allows the beam to be centered on the subtargets with a 50 μm accuracy. The interaction rate is monitored by three scintillator telescopes pointing at 90^o to the target.

In the $p-W$ setup, the target region is completely modified, as compared to the segmented active target system used in $S-U$ collisions. It consists of 5 tungsten subtargets each 2.0 cm thick ($\approx 1\ \lambda_{int}$) and 0.2 cm radius. They are 2.5 cm apart from each other in order to minimize reinteractions of secondaries and multiple scattering of muons inside the target itself. The electromagnetic calorimeter is removed and a long hadron absorber (15.6 cm of beryllium oxyde followed by 540 cm of carbon) starts right behind the target. Neither is the transverse neutral energy measured, nor is the subtarget identified. Since the 200 GeV/c proton beam is produced on a primary beryllium target, two gas Cerenkov counters are used to select the incident protons from contaminating pions. An ionization chamber is used to count the secondary beam.

In the 1990 sulphur run, the incident intensity was of $1.8\cdot 10^7$ S ions/burst, with an effective spill of about 3.3 sec. During the 1988 proton run, with an intensity of $4.5\cdot 10^7$ particles/burst, the number of identified pions corresponds to 33% of the total number of beam particles. The live time of the experiment is about 90% for the highest intensity

[1)] The energy detected by the calorimeter leads to an estimate of the total transverse energy released in the reaction in the pseudo-rapidity interval $1.7< \eta <4.1$. The relative error of this measurement is proportional to $1/\sqrt{E_T^0}$; for an energy of 90 GeV, it amounts to 12% and 16% respectively in the J/ψ and present configurations of the calorimeter [4].

$S-U$ runs and practically 100% for the $p-W$ data.

3 DATA ANALYSIS

A total of $4.3 \cdot 10^6$ ($4.5 \cdot 10^5$) dimuon triggers were collected in $S-U$ ($p-W$) interactions. After reconstruction, application of quality cuts and selection criteria, a sample of $5.0 \cdot 10^5$ ($8.1 \cdot 10^4$) events is available for the $S-U$ ($p-W$) analysis, as shown in Table 1. With some exceptions, which are described below, the cuts applied to the data presented in this paper are those used in [3].

In $S-U$ collisions, an event is selected if one and only one interaction occurred, i.e. one and only one incoming ion is detected by the beam hodoscope within the 20 ns reading gate and no secondary interaction recognized by the active target. Each event is then corrected for vertex identification inefficiency. This correction is a function of the collision centrality (and is thus applied on an event by event basis), as deduced from the calorimetry measurement. However, for very peripheral collisions, the subtarget identification algorithm in the present target system has a low efficiency, so that events with E_T^0 <10 GeV are rejected [2)]. In the $p-W$ case, dimuon reconstruction demands only one vertex and forces its location at the center of the target for the event reconstruction.

The analysis is done in the rapidity interval $3.0 \leq y_{\mu\mu} \leq 4.0$ and $P_{T\mu\mu} \geq 0.6$ GeV/c, which ensures an acceptance greater than 1% in the dimuon mass and transverse momentum regions considered. In order to take into account correlations between mass, dimuon's transverse momentum and transverse energy of the reaction, data are divided in approximately equipopulated intervals: five in P_T and four in E_T^0 [5]. In the case of proton-induced reactions, no electromagnetic calorimeter is used and the analysis is done on the integrated E_T^0 distribution[3)].

The signal dimuon mass and P_T distributions are obtained after a multidimensional background subtraction procedure in M, P_T, E_T^0 (M, P_T) for $S-U$ ($p-W$) data, as described hereafter. The combinatorial background originating from uncorrelated decays of pions and kaons is determined from our experimental like-sign muon pair distributions $N^{\mu^+\mu^+}$ and $N^{\mu^-\mu^-}$, according to

$$N_{bg}^{+-} = 2\ R\ \sqrt{N^{\mu^+\mu^+} N^{\mu^-\mu^-}} \quad . \tag{1}$$

This formula is a good estimate of the background provided that the acceptance of a muon is independent of its charge. This is obtained by applying specific geometrical cuts. Concerning the normalization, for high multiplicities the factor R is one. According to a Monte Carlo simulation of the background in the NA38 detector, based on the Fritiof event generator [6], the value of R is indeed $1.00 \pm 0.05 \pm 0.05$ for sulphur-induced reactions with E_T^0 >10 GeV and $1.25 \pm 0.10 \pm 0.05$ for proton events, where multiplicities are small. By using proton data obtained with two setups where the amount of absorbers is very different, the latter quoted R value is confirmed. The subtraction requires a minimum of 10 events per cell in order to avoid an underestimation of the background due to $N^{\mu^+\mu^+}$ or $N^{\mu^-\mu^-}$ low statistics bins. Finally, the restriction of the rapidity interval to $3.0 \leq y_{\mu\mu} \leq 4.0$ ensures the same decay path for all mesons.

An additional source of dimuon background, which is not taken into account by the subtraction formula (1), is the correlated $\pi^+\pi^-$ and K^+K^- pair production with

---

2) This cut selects collisions with an impact parameter smaller than approximately 9 fm.

3) In this case the number of nucleon-nucleon collisions is small and subject to large fluctuations. The neutral transverse energy E_T^0 is therefore weakly correlated to the geometry of the interaction.

subsequent decay into muons. Their contribution to the dimuon signal depends on the meson decay path in the apparatus. Experimental tests with a proton beam allowed to modify the distance from the target to the absorbers, as well as their interaction length and showed changes of the order of 5% in the dimuon signal in the 1.2 – 2.5 GeV/c^2 mass region, where the background is the highest as compared to the signal. This experimental result rules out a significant contribution from correlated $\pi^+\pi^-$ and K^+K^- pairs and gives further confidence in the uncorrelated background estimate described above. Furthermore, the decay $\phi \to K^+K^- \to \mu^+\mu^-$ has a negligible contribution to the dimuon spectrum, less than 1% when normalized to ϕ prompt decay into muons, because the kaon decay probability in our apparatus is very low (10^{-3} – 10^{-2}) [6]. A similar analysis shows that the decay $\rho \to \pi^+\pi^- \to \mu^+\mu^-$ is also negligible, as the reconstructed dimuon mass obtained by this mechanism lies below the ρ mass where the detector acceptance is $< 1\%$.

In Fig. 2 are presented the signal dimuon mass spectra measured in $p-W$ and $S-U$ collisions. The signal to background ratio amounts to 14.3 (6.7) in the $\rho+\omega$ (ϕ) resonance region for proton interactions. Although there is a significant increase of the background level in sulphur interactions, the signal to background ratio is still reasonable under the resonances: 1.3 (0.5) in the $\rho+\omega$ (ϕ) region.

A Monte Carlo simulation, described hereafter, is used to determine the acceptance and smearing matrices in two dimensions (with 50 MeV/c^2 bins in $M_{\mu\mu}$ and five bins in $P_{T\mu\mu}$).

The dimuon mass distribution is generated according to

$$\frac{dN}{dM_{\mu\mu}}|_{\Delta P_T} = A_\rho\ BW_\rho + A_\omega\ BW_\omega + A_\phi\ BW_\phi + A_C\ exp(-b\ M_{\mu\mu}) \qquad (2)$$

where the resonances are parametrized with classical Breit-Wigner distributions with mass and natural width values given by PDG [7]. The exponential term accounts for the continuum contribution: Dalitz decays ($\eta \to \mu\mu\gamma$, $\eta' \to \mu\mu\gamma$, $\omega \to \mu\mu\pi^0$) [8], semileptonic decays of $D\bar{D}$ correlated pairs and Drell-Yan production. The transverse momentum dimuon distribution depends on its mass and is described by $\frac{dN}{dP_{T\mu\mu}} \propto P_T\ exp(-c\ P_T)$, with $c = f(\frac{1}{M_{\mu\mu}})$ deduced from other dimuon measurements [9]. For the rapidity dependence, the charged particle distribution measured by other heavy ion experiments is used [10]. The polar variable θ in the Collins-Soper frame is described by the $1+cos^2\theta$ distribution [4]. An uniform distribution is taken for the azimuthal angle φ.

The initially chosen dimuon mass, transverse momentum and rapidity distributions are adjusted to the experimental data applying weights in each kinematical bin, using an iterative procedure. The convergence is obtained when the modified distributions tracked through the detector agree with the experimental data [5].

With these new distributions we obtain the correct acceptance and smearing matrices to be applied to the experimental data. As an example, Fig. 3 shows the mass dependence of the acceptance for dimuons produced in $p-W$ collisions in three of the five P_T regions. Similar values are obtained in $S-U$ reactions. The mass resolution σ is about 70 (90) MeV/c^2 at the ϕ resonance peak in the $p-W$ ($S-U$) setup. This is enough to separate the $\rho+\omega$ system from the ϕ resonance, although the ρ and ω resonances cannot be resolved.

[4] The shape of $1+cos^2\theta$ distribution does not differ significantly in the acceptance region of the detector from a flat $cos\theta$ distribution (a small a posteriori correction is applied, where appropriate, when computing the cross-sections) [5].

The numbers of $\rho+\omega$ and ϕ events, in each P_T and E_T^0 region, are obtained from maximum likelihood fits applying (2) to the corrected experimental dimuon mass distributions in the range $0.35 \leq M_{\mu\mu} \leq 2.5$ GeV/c^2, with a 50 MeV/c^2 bin width chosen to be of the order of the experimental mass resolution. The ρ and ω cross-sections are assumed to be equal [11] and their decay branching ratios into muons are taken from measurements in the e^+e^- decay channel [7], which leads to $A_\omega/A_\rho = 1.7 \pm 0.2$. Other considerations related to this normalization will be discussed later on. Thus, there are four free parameters in the fits, the normalizations of the ρ, ϕ and continuum contributions and the slope parameter b describing the continuum shape. The $\frac{\chi^2}{NDF}$ values lie between 1 and 2. In general, the ρ and ϕ contributions have practically no correlation in the fit (less than 3%). The ϕ and continuum components have correlations in the range of 5 to 10%. Due to the large natural ρ resonance width, the correlation between its contribution and the continuum amounts to 20 to 30%. Fig. 4 shows a typical fit to the dimuon mass cross-section in $p-W$ interactions, for a given P_T interval.

4 SYSTEMATIC ERRORS

The sources of systematic errors are discussed hereafter and summarized in Table 2.

- ▷ The estimated 5% systematic uncertainty for the R multiplicative factor used in the background subtraction formula (1) leads to a 1% uncertainty in the number of $\rho+\omega$ and ϕ signal events in proton interactions. In the sulphur case, the uncertainty on R results in a systematic error of 2% (5%) in the number of $\rho+\omega$ (ϕ) signal events.
- ▷ The differences between the Monte Carlo and experimental data distributions in mass, transverse momentum and rapidity of the dimuon lead to a 10% (5 – 7%) systematic error in the determination of the acceptance and smearing of the spectrometer in the $\rho+\omega$ (ϕ) mass region.
- ▷ A comparison of the experimental and Monte Carlo distributions of the vertex reconstructed coordinate along the beam axis shows that interactions of secondary charged particles in the absorbers contribute less than 2% in the $\rho+\omega$ and ϕ mass regions.
- ▷ The fitting procedure is a source of uncertainty:
  - The classical Breit-Wigner shape used in equation (2) is a good approximation for the ω and ϕ resonances, due to their small natural widths, but for the ρ finite-width additional corrections may have to be taken into account [12, 13]. The different fitting functions give somewhat different but statistically compatible results [5]. Although a more detailed treatment of the ρ line shape does not appear to be useful in our case, a systematic uncertainty of 10% is included in the number of $\rho+\omega$ events.
  - It has been pointed out that as the ρ and ω masses are nearly equal, interference phenomena may occur [14]. In our analysis we do not take them into account, as we are not sensitive to any mass shift due to our mass resolution.
  - In order to take into account the experimental uncertainty on the ρ and ω branching ratios (3 and 5%) as well as on the ω/ρ cross-section ratio (about 10%), studies are performed constraining the fit to different A_ω/A_ρ normalizations. On the other hand, it has been pointed out that information on the fireball lifetime could be obtained studying the ω/ρ ratio as a function of the energy density reached in relativistic nuclear collisions [15]. When we change A_ω/A_ρ from 1.7 to 0.85, the observed numbers of $\rho+\omega$ events are all compatible within statistical errors, leading in the most extreme case to a 6% difference.

In all these cases, the number of ϕ events remains practically unaffected, because the fit correlation between ϕ and ρ, ω contributions is negligible.

▷ The uncertainty on the absolute normalization is taken into account as follows:

- In $p-W$ ($S-U$) reactions, the luminosity measurement has a 2% (3%) uncertainty due to the target thickness and a 5% (2%) error related to beam intensity and trigger efficiencies. In addition, the sulphur beam absorption in the Beam In detector leads to a 0.8% systematic uncertainty.
- In the sulphur data, a 3% error on the vertex identification efficiency is estimated.
- The uncertainty due to the pion contamination in the proton beam leads to a 10% error.

Adding up quadratically all these systematic errors one obtains an uncertainty of $\pm 19\%$ ($\pm 16\%$) on the number of $\rho+\omega$ events and $\pm 14\%$ ($\pm 11\%$) on the number of ϕ events in proton (resp. sulphur) collisions.

5 RESULTS AND CONCLUSIONS

The dimuon yield normalized to the number of incident particles is obtained according to

$$\frac{d\sigma}{dM_{\mu\mu}} = \frac{1}{N_{inc}} \cdot \frac{dN^{corr}}{dM_{\mu\mu}} \cdot \frac{A_{tgt}}{l_{eff}\ N_A\ \rho_{tgt}} \tag{3}$$

where dN^{corr} is the number of dimuon events in the interval $dM_{\mu\mu}$= 50 MeV/c^2, corrected for acceptance and smearing, and for trigger and reconstruction efficiencies; N_{inc} is the number of incident particles in the target; l_{eff}, ρ_{tgt} and A_{tgt} are the effective lenght, density and mass number of the target. In sulphur runs, only the first subtarget has transverse dimensions bigger than the beam; a normalization to subtarget 1 is done as described in [6].

The main parameters providing the normalization factor for both reactions (integrated beam intensity, effective target thickness, trigger efficiency) are listed in Table 3.

Fig. 5 shows, for five P_T intervals, the dimuon mass cross-sections $d\sigma/dM_{\mu\mu}|_{\Delta P_T}$, measured in $p-W$ and $S-U$ collisions at 200 GeV/nucleon, in the intervals 3.0$\leq y_{lab} \leq$4.0 and $|\ cos\theta_{CS}\ |\leq$0.75. The spectra are integrated on the transverse energy distribution, taking into account a 12% correction factor in the $S-U$ case, due to the E_T^0 >10 GeV cut explained above.

The $\rho+\omega$ and ϕ differential cross-sections times braching ratio into muons $B \cdot \frac{d\sigma}{dP_T}$ can be directly extracted from Table 4, which gives the partially integrated cross-sections in each P_T interval. The quoted errors are only statistical (see Table 2 for systematic uncertainties).

Comparing the meson cross-sections in p-W and S-U collisions and assuming the power law A-dependence $\sigma = \sigma_0(A_{beam} \cdot A_{target})^{\alpha}$, we obtain the values $\alpha_{\rho+\omega}$ and α_ϕ as a function of P_T, shown in Table 4 and Fig. 6 [5)].

The systematic errors, not shown in the figure and table, are estimated to be $\pm 10\%$ ($\pm 4\%$) for $\alpha_{\rho+\omega}$ (α_ϕ) and are P_T independent. We observe that $\alpha_{\rho+\omega}$ and α_ϕ exhibit a similar increase with increasing P_T, which has been observed in past hadron-nucleus

[5)] It should be pointed out that the rapidity distributions may differ from proton to sulphur collisons. Therefore, the α values obtained here, in the 3< y_{lab} <4 region, may differ from the values determined for the full rapidity domain. In particular, the rapidity distributions are shifted by less than 10% between proton and sulphur-induced reactions; this produces a decrease of <0.03 for the α value of all mesons when calculated for the whole rapidity domain.

experiments [9, 16] and is known as the Cronin effect [17]. We also note that α_ϕ is systematically higher than $\alpha_{\rho+\omega}$ and that the difference is independent from P_T. Integrating the $\rho+\omega$ and ϕ cross-sections in our kinematical domain, $P_T \geq$0.6 GeV/c, we measure $\alpha_{\rho+\omega} = 1.00 \pm 0.02 \pm 0.07$ and $\alpha_\phi = 1.23 \pm 0.03 \pm 0.05$, leading to $\Delta\alpha_{\phi,\rho+\omega} = \alpha_\phi - \alpha_{\rho+\omega} = 0.23 \pm 0.04 \pm 0.09$ (Table 4).

These results show a clear enhancement of the ϕ production in $S-U$ interactions as compared to p-W collisions, independent on the meson transverse momentum.

References

[1] Quark Matter'91, eds. T.C. Awes, F.E. Obenshain, F. Plasil, M.R. Stroyer and C.Y. Wong, Nucl. Phys. A544 (1992); Quark Matter'93, eds. E. Stenlund, H.A. Gustavson, A. Oskarson and I. Otterlund, Nucl. Phys. A566 (1994); Quark Matter'95, eds. A.M. Poskanzer, J.W. Harris and L.S.Scroeder, Nucl. Phys. A590 (1995).
[2] M.C. Abreu et al., Phys. Lett. B, in this issue.
[3] C. Baglin et al., Phys. Lett. B 220 (1989) 471; C. Baglin et al., Phys. Lett. B 255 (1991) 459.
[4] Thierry Chambon, PhD thesis, Université Blaise Pascal - Clermont II (1993), Unpublished.
[5] R. Ferreira, PhD thesis, Universidade Técnica de Lisboa (1993), Unpublished.
[6] M. C. Abreu et al., Z. Phys. C 55 (1992) 365; L. Peralta, PhD thesis, Universidade de Lisboa (1991), Unpublished.
[7] J. J. Hernandez et al., *Review of Particle Properties*, Phys. Lett. B 239 (1990) 1.
[8] T. Akesson et al., preprint CERN-PPE/94-140.
[9] G. Branson et al., Phys. Rev. Lett. 38 (1977) 1334.
[10] G. Vasseur, PhD thesis, Centre d'Etudes Nucléaires de Saclay, Note CEA-N-2626 (1989), Unpublished.
[11] M. Aguilar-Benitez et al., Z. Phys. C 50 (1991) 405; R. Singer et al., Phys. Lett. B 60 (1976) 385; Blobel et al., Phys. Lett. B 48 (1974) 73.
[12] J. Canter et al., Phys. Rev. D 20 (1979) 1029.
[13] J. D. Jackson, Nuovo Cimento 34 A (1964) 1644.
[14] A. Chilingarov et al., Nucl. Phys. B 151 (1979) 29.
[15] U. Heinz and K. S. Lee, Phys. Lett. B 259 (1991) 162.
[16] J. Badier et al., Phys. Lett. B 122 (1983) 441.
[17] J.W. Cronin et al., Phys. Rev. D 11 (1975) 3105.
[18] M. Berenguer et al., Phys. Lett. B 332 (1994) 15.

List of Tables

List of Figures

	$p-W$	$S-U$
Triggers recorded	$4.5 \cdot 10^5$	$4.3 \cdot 10^6$
Reconstructed muon pairs	$4.3 \cdot 10^5$	$4.2 \cdot 10^6$
After selection criteria	$8.1 \cdot 10^4$	$5.0 \cdot 10^5$
Opposite-sign muon pairs	$7.2 \cdot 10^4$	$2.9 \cdot 10^5$
Like-sign muon pairs	$9.9 \cdot 10^3$	$2.1 \cdot 10^5$

Table 1: Data reduction.

	$p-W$		$S-U$	
	$\rho+\omega$	ϕ	$\rho+\omega$	ϕ
Background subtraction procedure	1	1	2	5
Monte Carlo distributions	10	5	10	7
Reinteractions	2	2	2	2
Fitting procedure	10	2	10	2
Absolute normalization	12	12	5	5
Total error	19	14	16	11

Table 2: Systematic errors (%) of the cross-section measurements.

	$p-W$	$S-U$
A_{tgt} (g)	183.85	238.03
ρ_{tgt} (g cm^{-3})	19.3	18.95
l_{eff} (cm)	6.21	0.845
N_{inc}	$(7.19\pm0.18)\cdot10^{11}$	$(1.67\pm0.02)\cdot10^{11}$
$< \epsilon_{BH} >$	0.79 ± 0.02	0.95 ± 0.01
$proton/total$	0.67	-
$< \epsilon_{rec} >$	0.99 ± 0.01	0.98 ± 0.01
ϵ_{trig}	0.94 ± 0.06	0.94 ± 0.06
live time	1.00	0.90 - 0.95
$\mathcal{L}$ (b^{-1})	$(1.85\pm0.13)\cdot10^{11}$	$(5.14\pm0.38)\cdot10^{9}$

Table 3: Main parameters used in cross-section calculations.

	$\sigma_{p-W}(\mu b)$		$\sigma_{S-U}(\mu b)$		α	
$\Delta P_T(GeV/c)$	$\rho+\omega$	ϕ	$\rho+\omega$	ϕ	$\rho+\omega$	ϕ
$0.6\leq P_T<0.9$	8.19±0.64	0.90±0.09	295.±30.	75.2±8.6	0.96±0.04	1.19±0.05
$0.9\leq P_T<1.15$	3.15±0.23	0.40±0.05	140.±12.	37.2±4.4	1.01±0.03	1.22±0.05
$1.15\leq P_T<1.35$	1.28±0.11	0.18±0.02	57.3±4.9	19.4±2.2	1.02±0.04	1.26±0.05
$1.35\leq P_T<1.65$	0.84±0.06	0.11±0.01	47.6±4.0	15.3±1.6	1.08±0.04	1.33±0.04
$1.65\leq P_T<3.0$	0.46±0.04	0.067±0.01	33.6±2.8	9.7±1.0	1.15±0.04	1.35±0.05
$0.6\leq P_T<3.0$	13.92±0.69	1.66±0.11	574.±33.	156.8±10.	1.00±0.02	1.23±0.03

Table 4: $B_{\rho\to\mu\mu}\sigma_\rho + B_{\omega\to\mu\mu}\sigma_\omega$ and $B_{\phi\to\mu\mu}\sigma_\phi$ (shortened here to "σ") in 3< y_{lab} <4 for p-W and S-U collisions at 200 GeV/c and A-dependence, in the quoted P_T intervals; division by the P_T interval widths would yield the corresponding differential cross-sections $Bd\sigma/dP_T$.

Figure 1: Low mass target region layout. a)$p-W$ setup: segmented target with 5×2 cm long W subtargets, followed by beryllium oxyde and carbon absorbers. b) $S-U$ setup: multiple active target system, with $10 \cdot 1$mm U, followed by Al_2O_3 and carbon absorbers, and the electromagnetic calorimeter.

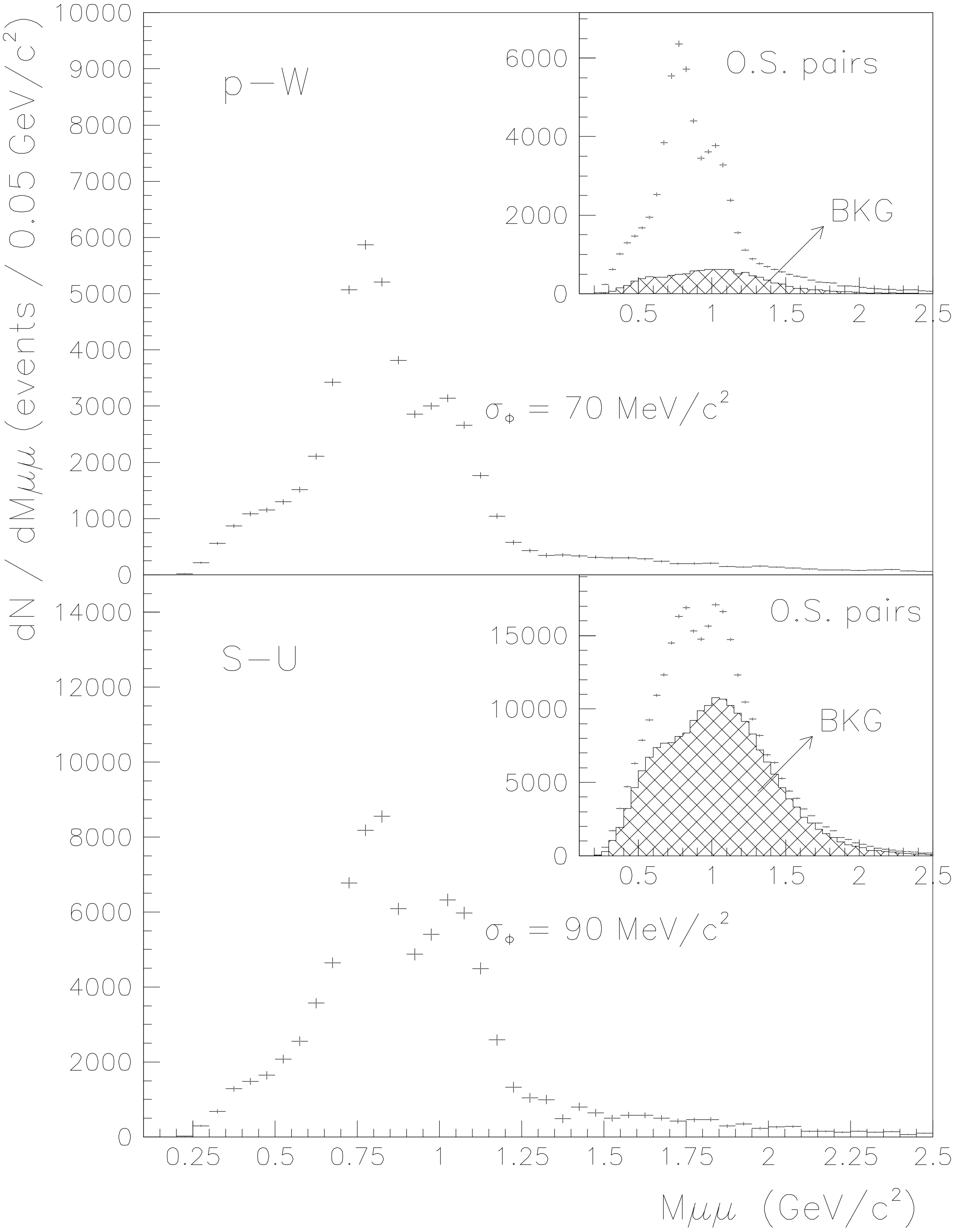

Figure 2: Dimuon mass distributions for low mass region in $p-W$ and $S-U$ interactions at 200 GeV/nucleon. σ_ϕ is the ϕ mass resolution. The insert shows the opposite sign and background distributions.

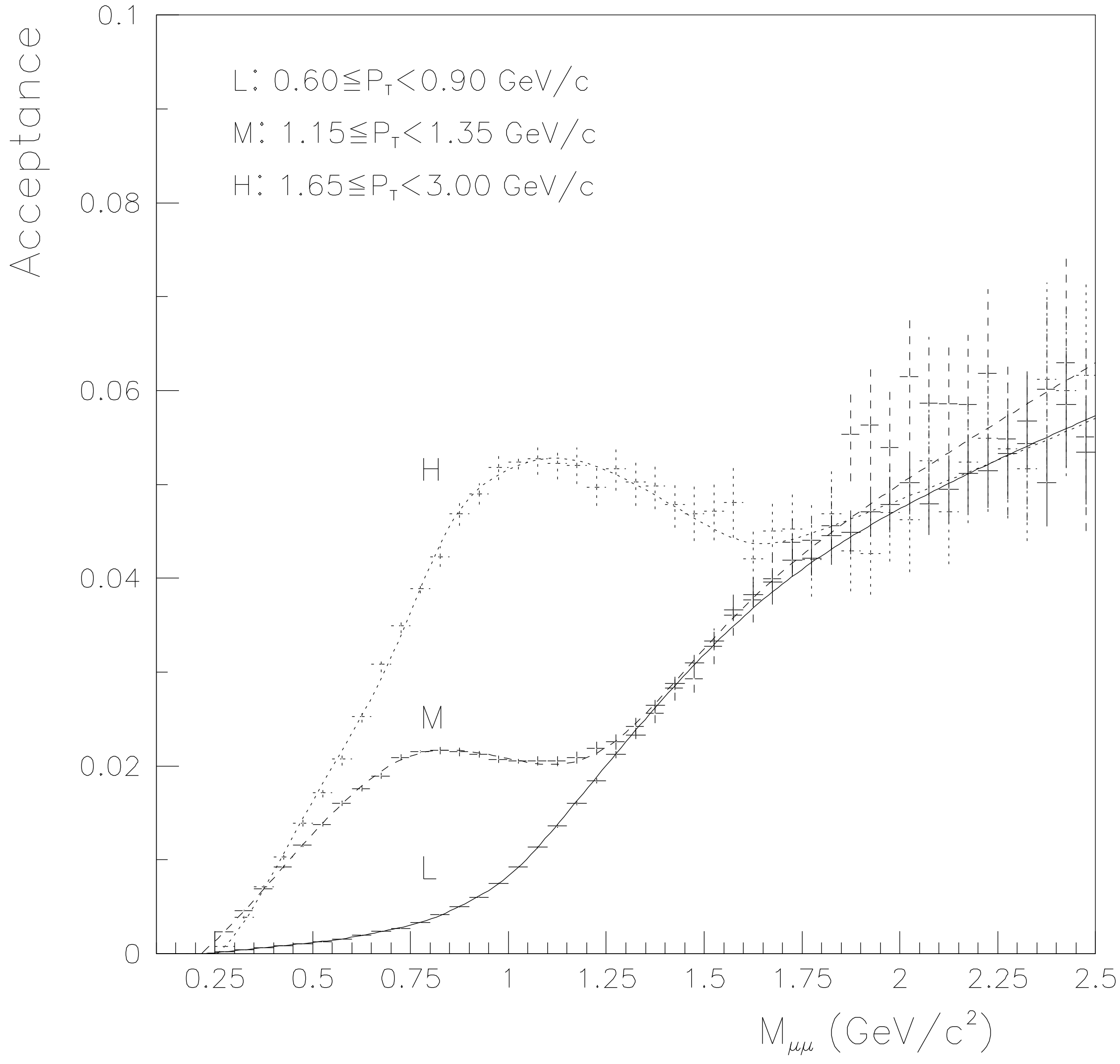

Figure 3: Dimuon acceptance as a function of mass for the lowest(L), middle(M) and highest(H) dimuon P_T intervals.

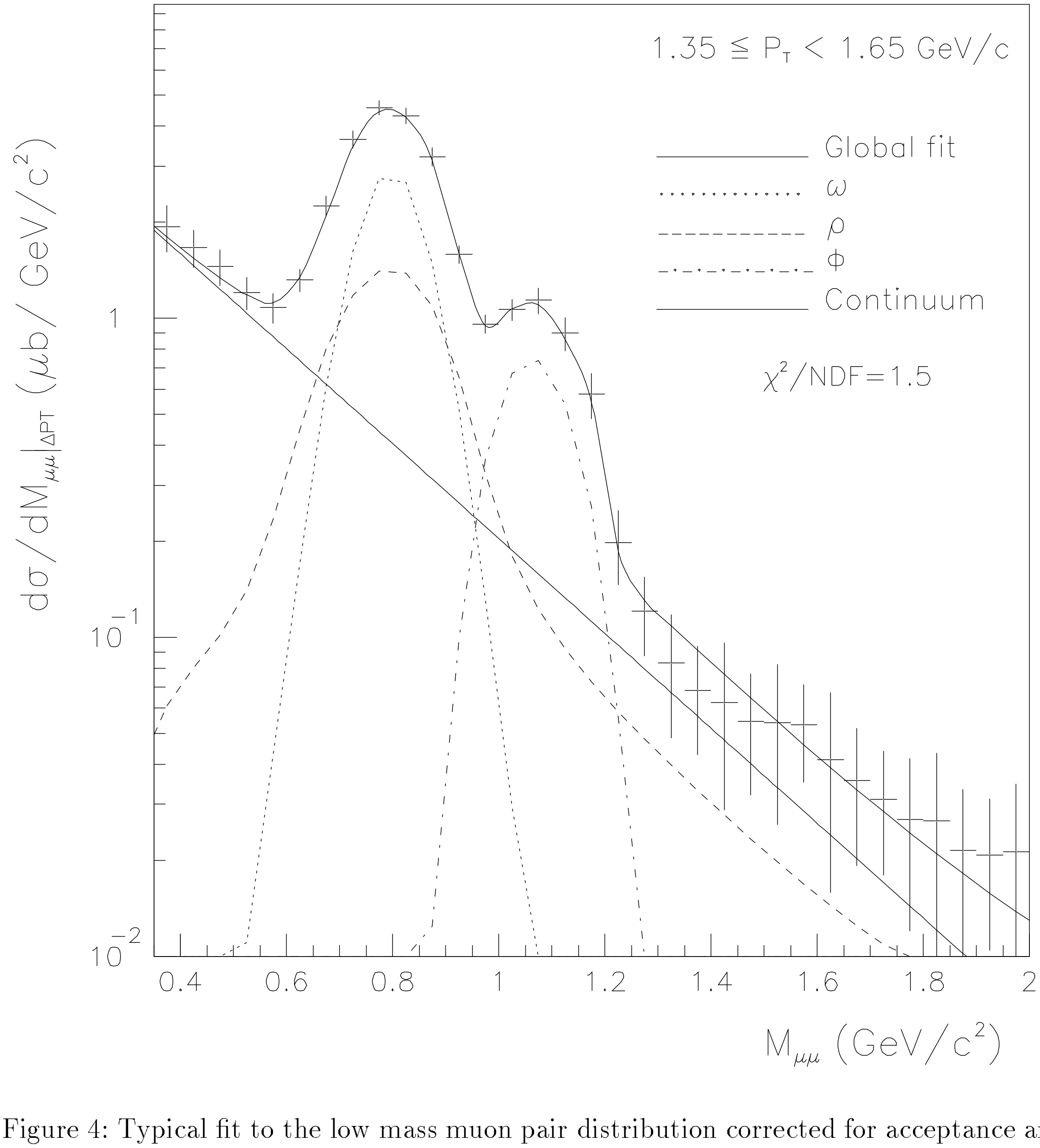

Figure 4: Typical fit to the low mass muon pair distribution corrected for acceptance and luminosity in $p - W$ collisions.

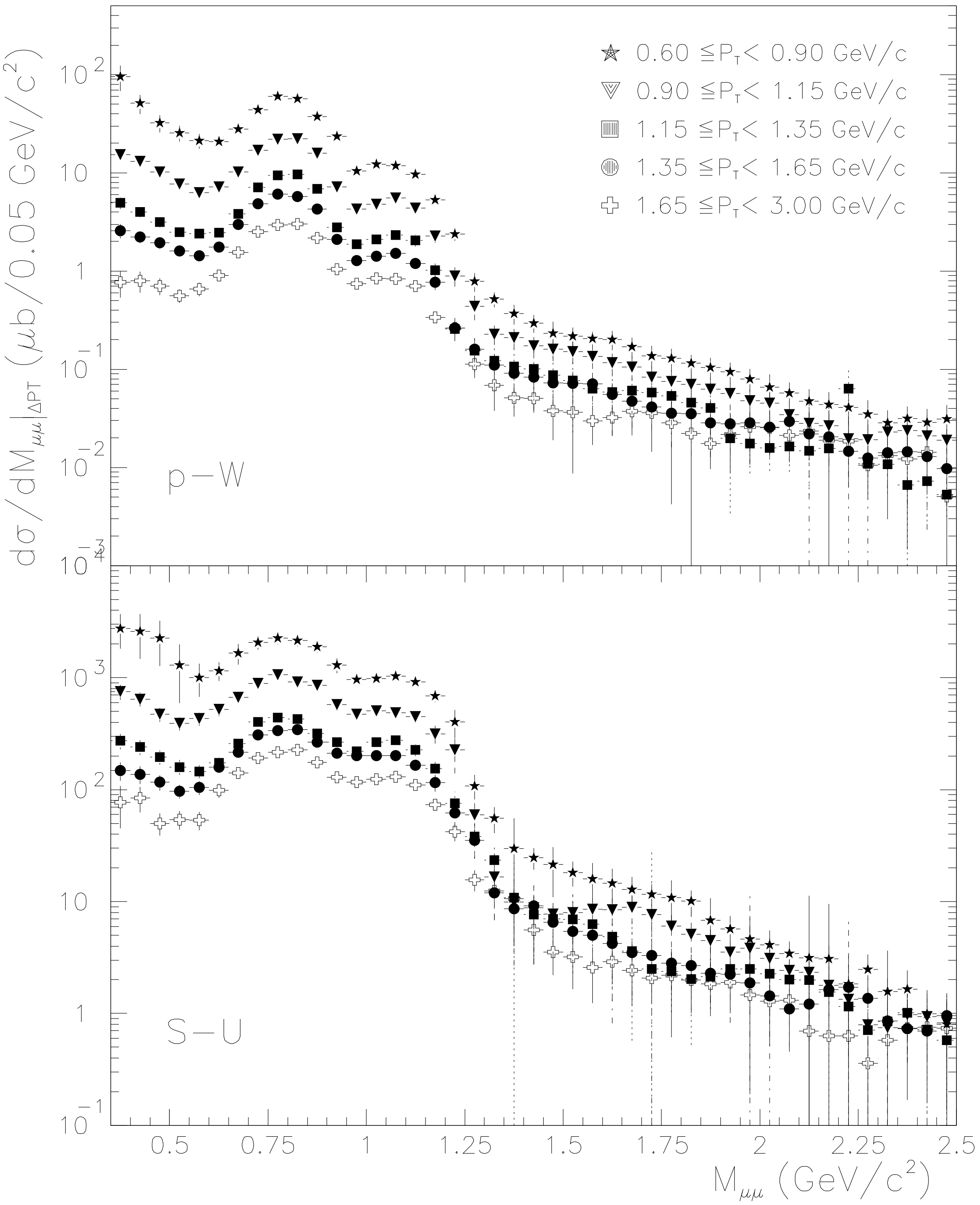

Figure 5: Low mass dimuon cross-section $d\sigma/dM_{\mu\mu}|_{\Delta P_T}$ (μb/0.05 GeV/c^2), in the intervals $3 \leq y_{lab} \leq 4$, $|\ cos\theta_{CS}\ | \leq 0.75$, measured in $p-W$ and $S-U$ collisions at 200 GeV/nucleon.

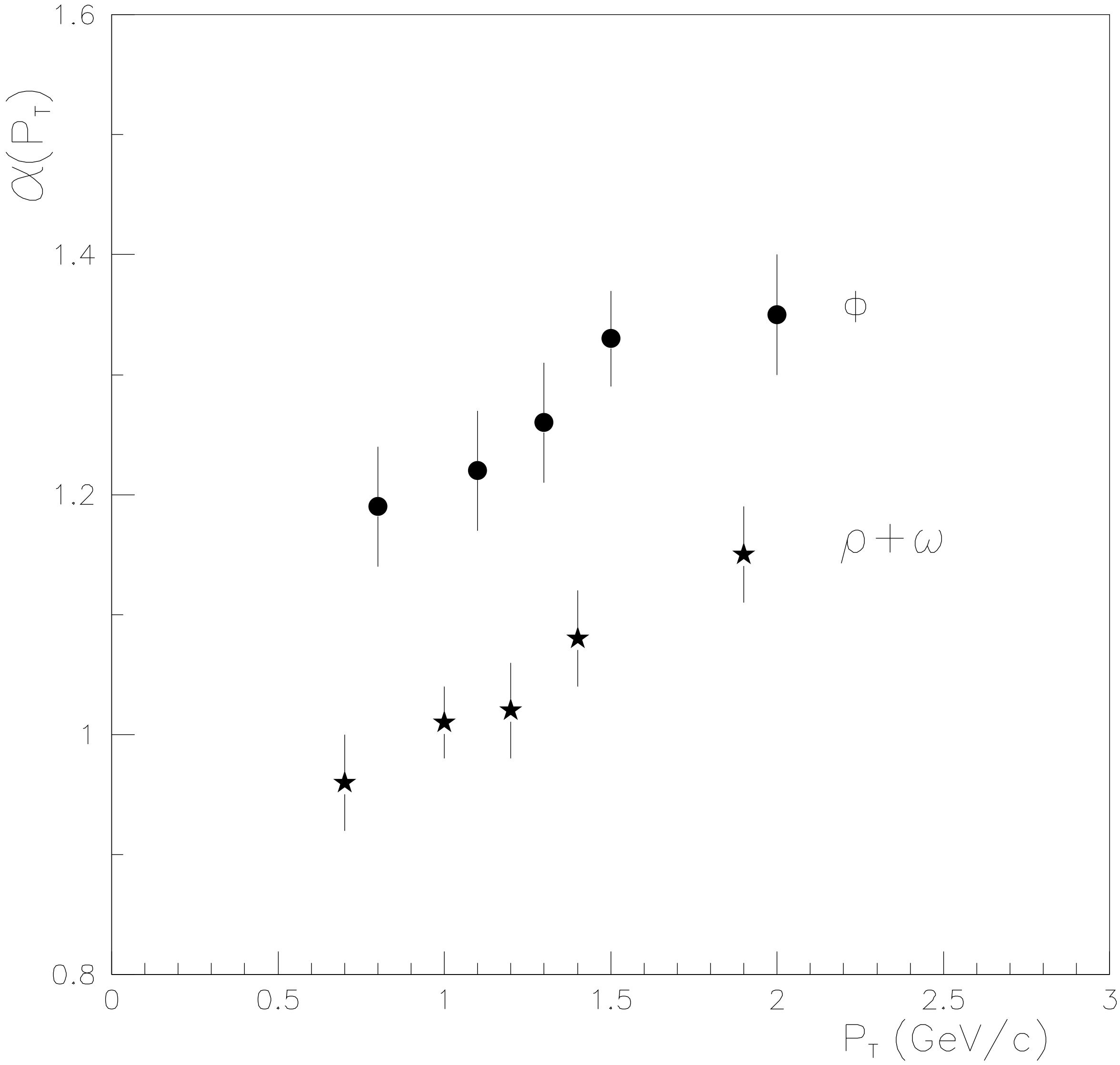

Figure 6: A-dependence of the resonances $\rho + \omega$ and ϕ as a function of the transverse momentum.